DOI: 10.1021/cg100728s

CRYSTAL GROWTH & DESIGN Article

2010, Vol. 10
3819–3823

Hydrothermal Synthesis of a B-Site Magnetic Ruthenate Pyrochlore

Richard J. Darton,[†,§] Scott S. Turner,[†,∥] Jeremy Sloan,[‡] Martin R. Lees,[‡] and Richard I. Walton*[,†]

[†]*Department of Chemistry and* [‡]*Department of Physics, University of Warwick, Coventry, CV4 7AL, U.K.* [§]*Current Address: School of Physical & Geographical Sciences, Keele University, Staffordshire, ST5 5BG, U.K.* [∥] *Current Address: Chemical Sciences, University of Surrey, Guildford, Surrey, GU2 7XH, U.K.*

Received June 1, 2010; Revised Manuscript Received June 28, 2010

ABSTRACT: The pyrochlore oxide $(Ce^{IV}_{0.67}Na_{0.33})_2Ru^{IV}_2O_7$ crystallizes directly as a phase-pure sample, without the need for postsynthesis annealing, from aqueous solutions of Ru^{3+}, Ce^{3+}, and sodium hydroxide in the presence of hydrogen peroxide as oxidizing agent at less than 250 °C. The structure has been refined using powder neutron diffraction and is consistent with electron diffraction and EDXA analysis performed using transmission electron microscopy (cubic $Fd\bar{3}m$ with $a = 10.1659(1)$ Å). The pyrochlore phase is metastable and upon heating to ~400 °C begins to phase separate to ultimately yield a mixture including $Na_2Ru_4O_9$, RuO_2, Ce_2O_3, and CeO_2. Magnetization measurements confirm that the material is a new example of a B-site magnetic pyrochlore, analogous to the known phase $Y_2Ru_2O_7$, but that show evidence for magnetic frustration at low temperatures. Heat capacity measurements and low-temperature neutron diffraction indicate the possibility of spin-glass-like behavior with no evidence of long-range magnetic order achieved at low temperature.

1. Introduction

The exploration of mild reaction conditions is an extremely attractive way in which to search for novel oxide-based, solid-state materials.[1,2] This is because traditional synthesis routes employ extreme temperatures to force interparticle diffusion between solid reagents, therefore usually allowing only the most thermodynamically stables phases to be isolated. Various *chimie douce*[3] methods have now been successfully employed in the preparation of solids and, in particular, widely applied for isolating oxides: these include coprecipitation, sol−gel processing, molten fluxes as reaction media, and topochemical transformation of solid precursors.[4] These methods often involve several steps in synthesis, such as the firing step of a disordered precursor, and this may impart a lack of control over crystallization. The hydrothermal method offers a very attractive one-step method for the isolation of oxides; this is well-known in silicate[5] and phosphate chemistry,[6] and that, although it has been extended to mixed-metal oxides, is less widely developed for such dense phases.[7−10] Typically, the mixed oxides prepared so far by this method have been already-known phases, and the advantage of solution synthesis has been in the control over crystal form to give well-defined morphology. This includes a number of important perovskite materials, such as $BaTiO_3$,[11] $PbZr_{1-x}Ti_xO_3$,[12] and $Na_{1-x}K_xNbO_3$[13] whose synthesis would usually be associated with the traditional high temperatures used in solid-state chemistry. For these materials hydrothermal synthesis can allow the deposition of thin films[14−16] or the controlled formation of nanocrystalline powders of the materials with shapes varying from spherical to anisotropic forms, such as plates or rods.[17−20]

In some cases, the isolation of new oxide phases, not seen at high temperatures, has proved possible using hydrothermal synthesis. This has included a layered strontium vanadate,[21] a novel superconducting bismuthate perovskite,[22] a metastable ilmenite polymorph of $NaNbO_3$,[23] and in our own work, a Ce(IV)-containing titanate pyrochlore that has redox properties suitable for catalysis.[24] Given the similarity of crystal radii of octahedral Ru^{4+} with Ti^{4+} (0.760 and 0.745 Å, respectively[25]), we considered that it might be possible to target novel ruthenium oxide compositions using hydrothermal synthesis based on the success of the method in the crystallization of titanates. Previous work on the hydrothermal chemistry of ruthenates has included a complex mixed-valent pyrochlore $Pb_2Ru_{2-x}Pb_xO_{6.5}$,[26] poorly crystalline, hydrous ruthenium dioxide with tin doping formed by hydrothermal hydrolysis of chlorides,[27] and lithium,[28] calcium[29] or barium[30] ruthenates prepared using high-temperature (>600 °C) and high-pressure (150 MPa) hydrothermal synthesis. In general, however, no systematic study of the hydrothermal chemistry of precious metals and their oxide products has been undertaken. Oxides of ruthenium have important applications in redox catalysis and electrochemistry,[31−34] and hence, the investigation of the preparation of new ruthenium oxides, which may also contain other redox-active metals, has some technological relevance. In this paper, we describe the successful synthesis of a phase-pure sample of a hitherto unknown complex ruthenium oxide under subcritical hydrothermal conditions, where solution synthesis conditions allow tuning of specific metal oxidation states in the product to yield a functional material, in this case characterized by its magnetic properties.

2. Experimental Section

The compound $(Ce_{0.67}Na_{0.33})_2Ru_2O_7$ was prepared under hydrothermal conditions where nominal molar ratios 1.0 $RuCl_3 \cdot 4H_2O$: 0.53 $CeCl_3 \cdot 7H_2O$/21 NaOH/37 H_2O_2/398 H_2O were used based on 0.25 g of $RuCl_3.4H_2O$. Note that the hydrated ruthenium chloride precursor readily takes up water from the air, as shown by repeated TGA analysis of our precursor, explaining the need for an apparent excess of this reagent. The reagents were stirred until homogeneous and heated in a sealed, Teflon-lined steel autoclave at 225 °C for

*To whom correspondence should be addressed. E-mail: r.i.walton@warwick.ac.uk.

Published on Web 07/15/2010

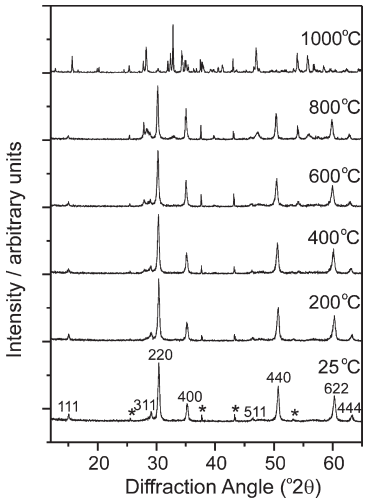

Figure 1. Powder XRD measured from the pyrochlore phase at room temperature and in situ upon heating to 1000 °C. The Miller indices correspond to the $Fd\bar{3}m$ pyrochlore unit cell, and the asterisks denote peaks from the alumina sample holder. For assignment of the peaks in the phase-separated product, see Supporting Information.

5 days to yield a black powder, which was recovered by filtration and washed with distilled water. No postsynthesis annealing is performed: the material is fully crystallized in its as-made form. Oxidizing conditions (the use of hydrogen peroxide) are necessary for the isolation of the new phase, otherwise mixtures of binary oxides are formed. The alternative approach to synthesis is to use $KRuO_4$ as oxidant and reagent, in place of the H_2O_2 and $RuCl_3 \cdot 4H_2O$. The use of a highly concentrated NaOH solution is required to produce well-crystallized samples of the material: at lower NaOH concentrations, poorly crystalline samples of the material were produced, and the same was true if the temperature was lowered below 200 °C. The use of a large excess of NaOH meant that no compositional variants could be isolated despite varying Ru and Ce ratios in exploratory reactions.

Powder X-ray diffraction analysis was performed using a Bruker D5000 powder X-ray diffractometer operating with Cu Kα radiation and fitted with an MRI TC-Basic furnace for measurements above room temperature, where alumina sample holders were used. Thermal analysis was performed on a Mettler Toledo TGA/DSC 1 from 30−900 at 10 °C min^{-1} in flowing air, with ∼10 mg sample heated in an alumina crucible. TEM experiments were performed using a JEOL 3000F HR-TEM instrument. Ru K-edge XANES spectra were measured on Station 9.3 of the Daresbury SRS in transmission mode from samples diluted with polyproplyene powder and pressed in ∼1 mm think pellets. The SRS (now permanently closed) operated with at 2 GeV with an average stored current of 2 mA. In our the incident X-ray energy was selected using a Si(111) double-crystal monochromator. Powder neutron diffraction experiments were made on the POLARIS diffractometer at ISIS, the U.K.'s spallation neutron source, from samples contained in thin-walled vanadium cans. Structural analysis of the neutron data was performed using the GSAS suite of software.[35] DC magnetization measurements were carried out using a Quantum Design Magnetic Property Measurement System (MPMS) squid magnetometer. The powder sample was placed in a gel capsule and mounted in a plastic straw. Heat capacity (C) measurements were performed using a Quantum Design Physical Property Measurement System (PPMS) calorimeter. The $C(T)$ data were collected using a 2τ relaxation method. The polycrystalline powder was pressed into the form of flat disk ($2.6 \times 2.6 \times 0.4$ mm^3) using a uniaxial press. The heat capacity of the empty sample platform and the grease used to attach the sample to the platform was collected prior to the measurement of the sample. The data were collected on cooling and between 50 and 10 K, points were taken every 1 K with a temperature rise of ∼2% of the set point temperature for each measurement.

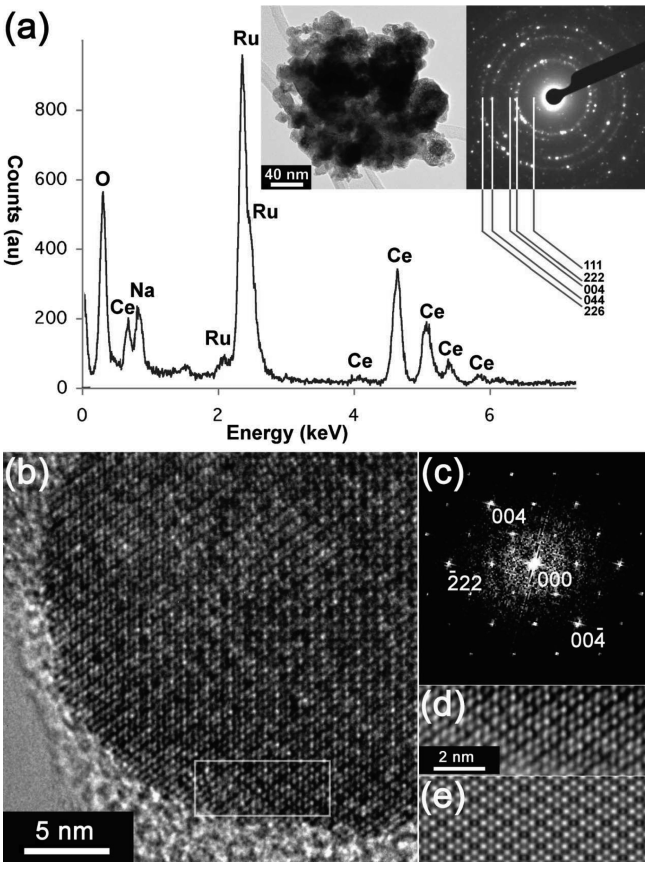

Figure 2. (a) The main figure shows an EDXA spectrum obtained from an agglomeration of ∼50 of the smallest crystallites of $(Na_{0.33}Ce_{0.67})_2Ru_2O_7$ (TEM image, left inset). Right inset shows an indexed SAED pattern from the same agglomerate. (b) HR-TEM image of a ca. 30 nm diameter particle showing a well-ordered microstructure. (c) FFT produced from (b) indexed according to a [110] projection of the $Fd\bar{3}m$ unit cell. Panels d and e show a detail from b and corresponding image simulation computed for the [110] projection and for −494 nm defocus using imaging parameters representative for the instrument used (i.e., 300 kV; C_s = 0.6 mm). Note that in b the sample is located on a background of amorphous carbon support; this accounts for some of the diffuse rings seen in c.

3. Results and Discussion

Powder X-ray diffraction revealed a phase-pure sample of a material with a pattern characteristic of a face-centered cubic $A_2B_2O_7$ pyrochlore.[36] The new pyrochlore is metastable with respect to collapse into binary and ternary oxides: variable-temperature XRD measurements show that phase separation begins as low as 400 °C with appearance of binary crystalline oxides of Ru and Ce along with $Na_2Ru_4O_9$, Figure 1 (see Supporting Information for phase identification after heating). TEM shows that the smallest crystallites of the new material are around 10 nm in diameter, although more typically 50 nm crystals are observed, Figure 2. This is consistent with Scherrer analysis of the powder XRD data that gave a typical average crystal dimension of 50 nm. Extended reaction periods were found to give no further increase in crystal size. Using the TEM, EDXA of 50 crystallites showed the presence of Na, Ru, and Ce in the oxide with a ratio of Na/Ce of ∼1:2 (Figure 2a). The TEM also showed the individual particles to be highly crystalline and SAED from regions of groups of crystals can be indexed on a face-centered cubic unit cell, consistent with the diffraction analysis below (see also Figure 2a and corresponding inset). High-resolution

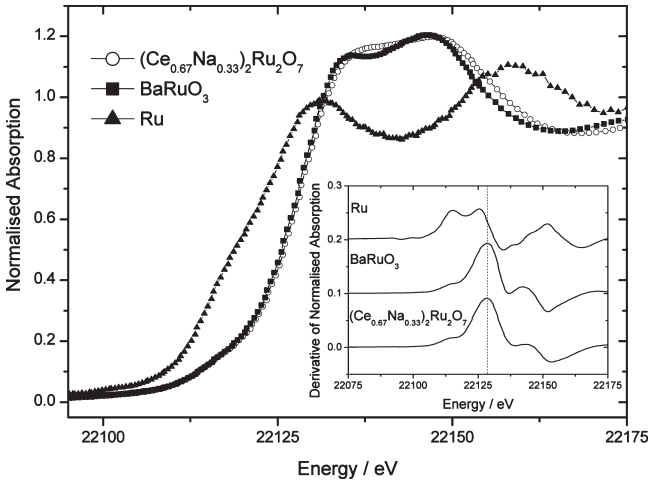

Figure 3. Ru K-edge XANES spectra. The inset shows the first derivative of the near-edge region where the dashed line indicates the position of the maximum in the curve for $(Na_{0.33}Ce_{0.67})_2Ru_2O_7$.

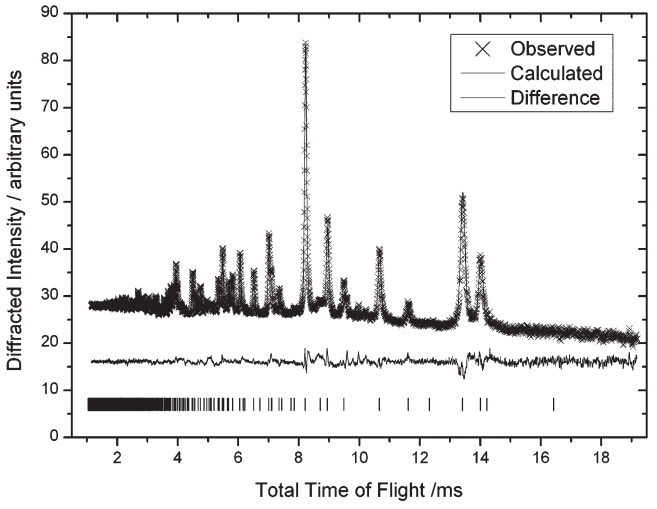

Figure 4. Rietveld refinement of powder neutron data (POLARIS A-bank at 4.2 K). The tick marks denote positions of Bragg peaks of $(Na_{0.33}Ce_{0.67})_2Ru_2O_7$ $Fd\bar{3}m$ a = 10.1652(4) Å.

TEM also reveals that individual crystallites of $(Ce_{0.67}Na_{0.33})$-Ru_2O_7 show a high degree of crystalline order (Figures 2b–e) that is consistent with the refined structural model described below.

The compositional information from laboratory powder XRD and TEM allowed a structural model to be constructed based on the known cubic pyrochlore $Y_2Ru_2O_7$[37–39] with the presence of both sodium and cerium(IV) on the A-site. The presence of cerium(IV) is anticipated by analogy with the related Ce(IV) phase $(Na_{0.33}Ce_{0.67})_2Ti_2O_7$, which also crystallizes from $CeCl_3$ in the presence of oxidizing H_2O_2.[24] The valence of ruthenium was measured by Ru K-edge XANES, Figure 3, where an edge shift from Ru metal characteristic of Ru(IV) is observed (12.6 eV) similar to $BaRu^{IV}O_3$ (12.4 eV) and the previously reported $La_2Ru^{IV}O_5$ (12.5 eV).[40] This shows that our new material is a new member of a family of cubic pyrochlores $M_2Ru^{IV}{}_2O_7$ ($M = Y^{3+}$ or Ln^{3+}).[41] For the Na–Ce–Ru material, although the A-site contains Ce(IV), the presence of sodium maintains charge balance, as shown by the EDXA analysis. The structure was then refined against powder neutron diffraction data; this allowed a reliable refinement of oxide ion content and position owing of the favorable contrast in coherent neutron scattering lengths of the constituent elements. Figure 4 shows a final Rietveld fit to the neutron data, and Table 1 the refined crystal parameters. The pyrochlore structure is known to accommodate various forms of disorder, including mixing of A and B site metals, migration of one oxide to a fluorite-type position and non-stoichiometry with oxygen deficiency or partial replacement of oxide by hydroxide, halide anions or water.[36] The best refined structural model for our material, however, gave close to an ideal pyrochlore structure, with composition $A_2B_2O_{7-\delta}$ and $\delta \approx 0$, as shown in Table 1. Although the presence of some hydroxide on the O2 site might be expected from the high pH we used in synthesis, none could be detected in the product using any technique (IR or TGA for example), and we also note the absence of any noticeable levels of background scatter due to the incoherent scattering of protons in our neutron diffraction data. The presence of chloride ions in the product is ruled out by the absence of any characteristic chlorine fluorescence in the EDXA spectra. In the final cycle of refinement the occupancies of the metal sites were fixed at values to achieve charge balance and their thermal parameters varied to give the final crystal structure shown in Table 1.

Table 1. Crystal Structure Parameters for $(Na_{0.33}Ce_{0.67})_2Ru_2O_7$ $Fd\bar{3}m$ a = 10.1659(1) Å at 4.2 K[a]

site	x	y	z	occupancy[b]	B_{iso}/Å^2
Na (16a)	0.5	0.5	0.5	0.3333	0.0153(5)
Ce (16a)	0.5	0.5	0.5	0.6667	0.0153(5)
Ru (16c)	0.0	0.0	0.0	1.0000	0.00004(4)
O1 (48f)	0.32330(9)	0.125	0.125	1.042(4)	0.00976(14)
O2 (8b)	0.375	0.375	0.375	0.97931(9)	0.0108(4)

[a] R_p = 0.0170, wR_p = 0.0131. [b] Occupancies of metal sites were fixed at the values stated after initial analysis (see text).

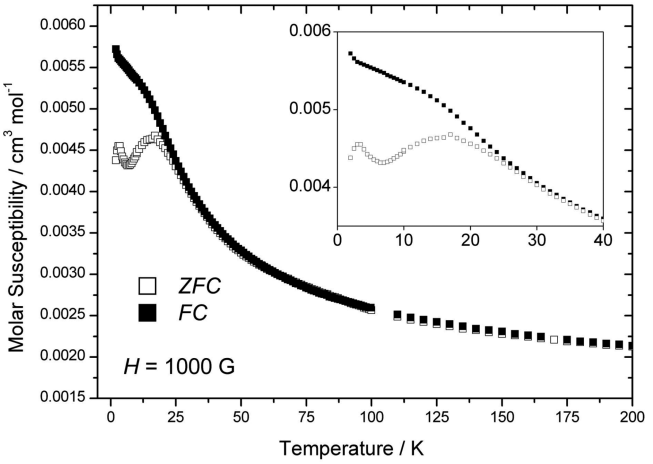

Figure 5. Temperature dependence of the molar magnetic susceptibility of $(Na_{0.33}Ce_{0.67})_2Ru_2O_7$ in zero-field-cooled (ZFC) and field-cooled (FC) conditions. The inset shows the low temperature region for clarity.

Magnetization data from the new Na–Ce(IV)–Ru(IV) phase, Figure 5, reveal magnetic frustration at low temperature, with distinct deviation of field-cooled and zero-field curves below ~28 K. This is consistent with the arrangement of Ru^{4+} spins over the tetrahedral B site sublattice of the pyrochlore structure.[42] Magnetization measurements were made under zero-field-cooled and field-cooled conditions with various external fields applied during the measurement. A magnetic transition to the frustrated state occurs at 28 K,

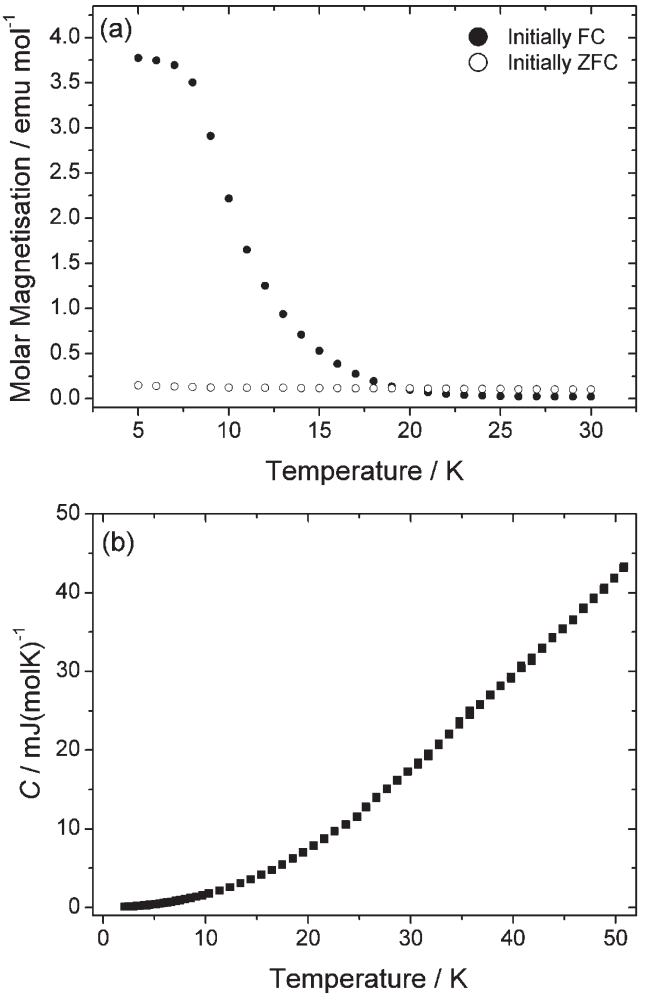

Figure 6. Plots of (a) remnant magnetization measured after cooling the sample in zero-field and after cooling in a field of 50 kG and (b) heat capacity versus temperature measured upon cooling the sample.

below which there is onset of magnetic ordering between the ruthenium centers; above 28 K, the sample behaves as a simple paramagnet. The measurement was repeated in external fields of 50 and 200 G resulting in little deviation of either the transition temperature or the observed temperature vs magnetic susceptibility curves. To confirm the frustrated nature of the phase below 28 K the sample was cooled to 5 K in zero field, a 50 kG external field was introduced and then reduced to zero, followed by measurement of the sample on warming into the paramagnetic phase, Figure 6a. This was repeated except with the sample initially being cooled in 50 kG field, rather than in zero field. A remnant magnetization persisted in zero magnetic field after the field-cooled process, but no remnant magnetization occurred after the zero-field-cooled process, consistent with a spin-frozen state. Finally, no magnetic hysteresis was observed at 5 K. The presence of magnetic frustration is consistent with the fact that we are studying a B-site magnetic pyrochlore, with spins located on the tetrahedral sublattice of the B sites.[42] However, the transition temperature for the compound reported here is significantly lower than for the closest analogue $Y_2Ru_2O_7$ (~80 K),[37−39] and the Weiss constant of −895 K is not as large as the value of −1100 K reported for the yttrium material (note that although the mean-field approach does not apply, this direct comparison is still a useful way of comparing the behavior of the two materials).[37−39] The transition temperature may be correlated with the cubic lattice parameter, since when Y^{3+} is exclusively replaced with the smaller ion Lu^{3+}, for example, *a* changes from 10.141 to 10.055 Å with an increase in transition temperature to 85 K.[37−39] The fact that the cell parameter for the Na/Ce compound is slightly larger at 10.165 Å is consistent with the observation of a lower transition temperature. For $(Ce_{0.67}Na_{0.33})Ru_2O_7$ there is further clear evidence for geometric magnetic frustration in other measurements: powder neutron diffraction shows no additional magnetic diffraction at low temperature (4.2 K) when the data are compared to those measured at room temperature (Supporting Information) and the heat capacity measured on cooling, Figure 6b, shows no feature that might be associated with spin ordering. Other B-site magnetic pyrochlores have been classified as spin glasses,[42] such as $Y_2Mo_2O_7$,[43] but for the ruthenates the situation is less clear. Although $Y_2Ru_2O_7$ described has been described as having a spin glass state at low temperature,[37,38] the presence of both strong magnetic Bragg peaks at 10 K and a distinct, sharp peak in the heat capacity on cooling shows that long-range order is achieved.[39,44]

4. Conclusions

In summary, we have illustrated the power of hydrothermal synthesis in the isolation of new complex oxides phases that would be difficult to prepare using conventional approaches. Particularly attractive is the control over metal oxidation state offered by use of solution reagents, allowing targeted synthesis of materials containing desired mixtures of metals in interesting oxidation states to yield functional materials. The high temperature XRD suggests that $(Ce_{0.67}Na_{0.33})_2Ru_2O_7$ would be impossible to prepare from its constituent oxides by traditional high temperature synthesis methods, and even if careful sintering of sol−gel precursors proved possible at low temperatures, it would involve a lengthy preparation, in contrast to the one-step hydrothermal approach we have developed. Although we have focused on the characterization of the magnetic properties of the new material and shown it to be distinct from known related phases prepared by solid-state methods, given the catalytic properties of ruthenium oxides, the material could also be of interest in other fields. Here, the small particle size could be beneficial, and in the area of redox catalysis the incorporation of two redox-active metals could produce some interesting activity: this is the focus of our current research.

Acknowledgment. We thank the EPSRC for funding this work (EP/F012721) and the STFC for provision of beamtime at the Daresbury SRS and at ISIS, where Dr Ian Harvey and Dr Ron Smith, respectively, helped with our experiments. Some of the equipment used in materials characterization at the University of Warwick was obtained through the Science City Advanced Materials project "Creating and Characterising Next Generation Advanced Materials" with support from Advantage West Midlands (AWM) and part funded by the European Regional Development Fund (ERDF). We are also indebted to the Department of Materials, Oxford, for access to the JEOL 3000F HR-TEM through the EPSRC equipment support fund. Johnson Matthey plc is acknowledged for loan of ruthenium salts, and we thank Dr David Thompsett and Dr Janet Fisher at the Johnson Matthey Technology Centre for useful discussions.

Supporting Information Available: Assigment of powder XRD and low temperature neutron diffraction. This information is available free of charge via the Internet at http://pubs.acs.org/.

References

(1) Jansen, M. *Angew. Chem., Int. Ed.* **2002**, *41*, 3747.
(2) Rosseinsky, M. J. *Angew. Chem., Int. Ed.* **2008**, *47*, 8778.
(3) Rouxel, J.; Tournoux, M. *Solid State Ionics* **1996**, *84*, 141.
(4) Gopalakrishnan, J. *Chem. Mater.* **1985**, *7*, 1265.
(5) Cundy, C. S.; Cox, P. A. *Chem. Soc. Rev.* **2003**, *103*, 663.
(6) Cheetham, A. K.; Férey, G.; Loiseau, T. *Angew. Chem., Int. Ed.* **1999**, *38*, 3268.
(7) Demazeau, G. *J. Mater. Chem.* **1999**, *9*, 15.
(8) Riman, R. E.; Suchanek, W. L.; Lencka, M. M. *Ann. Chim.* **2002**, *27*, 15.
(9) Walton, R. I. *Chem. Soc. Rev.* **2002**, *31*, 230.
(10) Modeshia, D. R.; Walton, R. I. *Chem. Soc Rev.* **2010**, *39* DOI: 10.1039/b904702f.
(11) Eckert, J. O.; Hung-Houston, C. C.; Gersten, B. L.; Lencka, M. M.; Riman, R. E. *J. Am. Ceram. Soc.* **1996**, *79*, 2929.
(12) Cheng, H. M.; Ma, J. M.; Zhu, B.; Cui, Y. H. *J. Am. Ceram. Soc.* **1993**, *76*, 625.
(13) Handoko, A. D.; Goh, G. K. L. *Green Chem.* **2010**, *12*, 680.
(14) Zhu, W.; Akbar, S. A.; Asiaie, R.; Dutta, P. K. *J. Electroceram.* **1998**, *2*, 21.
(15) Tan, C. K.; Goh, G. K. L.; Chi, D. Z.; Lu, A. C. W.; Lok, B. K. *J. Electroceram.* **2006**, *16*, 581.
(16) Goh, G. K. L.; Chan, K. Y. S.; Tan, B. S. K.; Zhang, Y. W.; Kim, J. H.; Osipowicz, T. *J. Electrochem. Soc.* **2008**, *155*, D52.
(17) Ohara, Y.; Koumoto, K.; Yanagida, H. *J. Am. Ceram. Soc.* **1994**, *77*, 2327.
(18) Feng, Q.; Hirasawa, M.; Yanagisawa, K. *Chem. Mater.* **2001**, *13*, 290.
(19) Cho, S.-B.; Oledzka, M.; Riman, R. E. *J. Cryst. Growth* **2001**, *226*, 313.
(20) Maxim, F.; Ferreira, P.; Vilarinho, P. M.; Reaney, I. *Cryst. Growth Des.* **2008**, *8*, 3309.
(21) Oka, Y.; Yao, T.; Yamamoto, N.; Ueda, M.; Maegawa, S. *J. Solid State Chem.* **2000**, *149*, 414.
(22) Jiang, H.; Kumada, N.; Yonesaki, Y.; Takei, T.; Kinomura, N.; Yashima, M.; Azuma, M.; Oka, K.; Shimakawa, Y. *Jpn. J. Appl. Phys.* **2009**, *48*, 010216.
(23) Modeshia, D. R.; Darton, R. J.; Ashbrook, S. E.; Walton, R. I. *Chem. Commun.* **2009**, 68.
(24) Wright, C. S.; Fisher, J.; Thompsett, D.; Walton, R. I. *Angew. Chem. Int Ed.* **2006**, *45*, 2442.
(25) Shannon, R. D. *Acta Cryst. A* **1976**, *32*, 751.
(26) Horowitz, H. S.; Longo, J. M.; Lewandowski, J. T. *Mater. Res. Bull.* **1981**, *16*, 489.
(27) Wang, C.-C.; Hu, C.-C. *Electrochem. Acta* **2005**, *50*, 2573.
(28) Soma, M.; Sato, H. *J. Phys. Soc. Jpn.* **2006**, 75.
(29) Munenaka, T.; Sato, H. *J. Phys. Soc. Jpn.* **2006**, 75.
(30) Ogawa, T.; Sato, H. *J. Alloy. Compd.* **2004**, *383*, 313.
(31) Ardizzone, S.; Falciola, M.; Trasatti, S. *J. Electrochem. Soc.* **1989**, *136*, 1545.
(32) Fachinotti, E.; Guerrini, E.; Tavares, A. C.; Trasatti, S. *J. Electroanal. Chem.* **2007**, *600*, 103.
(33) Malmgren, C.; Eriksson, A. K.; Cornell, A.; Backstrom, J.; Eriksson, S.; Olin, H. *Thin Solid Films* **2010**, *518*, 3615.
(34) Cheng, J. B.; Zhang, H. M.; Ma, H. P.; Zhong, H. X.; Zou, Y. *Electrochim. Acta* **2010**, *55*, 1855.
(35) Larson, A. C.; Dreele, R. B. V. *General Structure Analysis System* (*GSAS*), Los Alamos National Laboratory Report LAUR 86-748; Los Alamos National Laboratory: Los Alamos, NM, 1994.
(36) Subramanian, M. A.; Aravamudan, G.; Rao, G. V. S. *Prog. Solid State Chem.* **1983**, *15*, 55.
(37) Ito, M.; Yasui, Y.; Kanada, M.; Harashina, H.; Yoshii, S.; Murata, K.; Sato, M.; Okumura, H.; Kakurai, K. *J. Phys. Soc. Jpn.* **2000**, *69*, 888.
(38) Taira, N.; Wakeshima, M.; Hinatsu, Y. *J. Solid State Chem.* **1999**, *144*, 216.
(39) van Duijn, J.; Hur, N.; Taylor, J. W.; Qiu, Y.; Huang, Q. Z.; Cheong, S. W.; Broholm, C.; Perring, T. G. *Phys. Rev. B* **2008**, *77*, 020405.
(40) Arčon, I.; Benčan, A.; Kodre, A.; Kosec, M. *X-Ray Spectrom.* **2007**, *36*, 301.
(41) Kennedy, B. J.; Vogt, T. *J. Solid State Chem.* **1996**, *126*, 261.
(42) Gardner, J. S.; Gingras, M. J. P.; Greedan, J. E. *Rev. Mod. Phys.* **2010**, *82*, 53.
(43) Greedan, J. E.; Sato, M.; Xu, Y.; Razavi, F. S. *Solid State Commun.* **1986**, *59*, 895.
(44) Ito, M.; Yasui, Y.; Kanada, M.; Harashina, H.; Yoshii, S.; Murata, K.; Sato, M.; Okumura, H.; Kakurai, K. *J. Phys. Chem. Solids* **2001**, *62*, 337.